

## Friction Reduction Through Ultrasonic Vibration Part 2:

Sednaoui, Thomas; Vezzoli, Eric; Dzidek, Brygida Maria; Lemaire-semail, Betty; Chappaz, Cedrick; Adams, Michael

DOI:

[10.1109/TOH.2017.2671376](https://doi.org/10.1109/TOH.2017.2671376)

License:

Other (please specify with Rights Statement)

*Document Version*

Peer reviewed version

*Citation for published version (Harvard):*

Sednaoui, T, Vezzoli, E, Dzidek, BM, Lemaire-semail, B, Chappaz, C & Adams, M 2017, 'Friction Reduction Through Ultrasonic Vibration Part 2: Experimental Evaluation of Intermittent Contact and Squeeze Film Levitation', *IEEE Transactions on Haptics*, vol. 10, no. 2, pp. 208-216.  
<https://doi.org/10.1109/TOH.2017.2671376>

[Link to publication on Research at Birmingham portal](#)

### **Publisher Rights Statement:**

(c) 2017 IEEE. Personal use of this material is permitted. Permission from IEEE must be obtained for all other users, including reprinting/republishing this material for advertising or promotional purposes, creating new collective works for resale or redistribution to servers or lists, or reuse of any copyrighted components of this work in other works

### **General rights**

Unless a licence is specified above, all rights (including copyright and moral rights) in this document are retained by the authors and/or the copyright holders. The express permission of the copyright holder must be obtained for any use of this material other than for purposes permitted by law.

- Users may freely distribute the URL that is used to identify this publication.
- Users may download and/or print one copy of the publication from the University of Birmingham research portal for the purpose of private study or non-commercial research.
- User may use extracts from the document in line with the concept of 'fair dealing' under the Copyright, Designs and Patents Act 1988 (?)
- Users may not further distribute the material nor use it for the purposes of commercial gain.

Where a licence is displayed above, please note the terms and conditions of the licence govern your use of this document.

When citing, please reference the published version.

### **Take down policy**

While the University of Birmingham exercises care and attention in making items available there are rare occasions when an item has been uploaded in error or has been deemed to be commercially or otherwise sensitive.

If you believe that this is the case for this document, please contact [UBIRA@lists.bham.ac.uk](mailto:UBIRA@lists.bham.ac.uk) providing details and we will remove access to the work immediately and investigate.

# Friction Reduction Through Ultrasonic Vibration Part 2: Experimental Evaluation of Intermittent Contact and Squeeze Film Levitation

Thomas Sednaoui, Eric Vezzoli, Brygida Dzidek, Betty Lemaire-Semail, *Member, IEEE*, Cedrick Chappaz, and Michael Adams

**Abstract**—In part 1 of the current study of haptic displays, a finite element (FE) model of a finger exploring a plate vibrating out-of-plane at ultrasonic frequencies was developed as well as a spring-frictional slider model. It was concluded that the reduction in friction induced by the vibrations could be ascribed to ratchet mechanism as a result of intermittent contact. The relative reduction in friction calculated using the FE model could be superimposed onto an exponential function of a dimensionless group defined from relevant parameters. The current paper presents measurements of the reduction in friction, involving real and artificial fingertips, as a function of the vibrational amplitude and frequency, the applied normal force and the exploration velocity. The results are reasonably similar to the calculated FE values and also could be superimposed using the exponential function provided that the intermittent contact was sufficiently well developed, which for the frequencies examined correspond to a minimum vibrational amplitude of  $\sim 1 \mu\text{m}$  P-P. It was observed that the reduction in friction depends on the exploration velocity and is independent of the applied normal force and ambient air pressure, which is not consistent with the squeeze film mechanism. However, the modelling did not incorporate the influence of air and the effect of ambient pressure was measured under a limited range of conditions, Thus squeeze film levitation may be synergistic with the mechanical interaction.

**Index Terms**—Tactile devices and display, Tactile stimulator, Squeeze film effect, Ultrasonic devices, Friction modulation.

## 1 INTRODUCTION

THE friction of flat screens can be globally modulated by the application of ultrasonic vibration with varying amplitude to create the illusion of a texture [1]. An understanding of the mechanism of friction modulation would greatly facilitate design optimisation and it has been proposed recently that the mechanism involves a combination of squeeze film levitation and intermittent contact [2], [3]. In part 1 of the current work [4], the underlying principles of friction modulation arising from intermittent contact were elucidated by developing numerical models. Here, experimental data involving real and artificial fingertips will be presented in order to validate the modelling. In addition, the results of measurements carried out at reduced ambient pressure will be described, which establish that the contribution of squeeze flow levitation is at least not significant for the particular artificial finger employed in the current work.

### 1.1 Intermittent Contact

Optical measurements have revealed that intermittent contact resulting from ultrasonic vibration may be characterised by the phase shift between the vibrating plate and the skin surface dynamics of the exploring finger pad or probe [3], [4]. That is, for small vibrational amplitudes, contact persists but with increasing amplitude there is a transition regime in which intermittent contact develops with an increasing phase shift. Ultimately, for large amplitudes, the phase shift tends to an asymptotic value corresponding to the intermittent contact being fully developed. Such data were used to calibrate a finite element (FE) of the exploration process [4]. Data interpretation was assisted by the development of a simple elastic model of a finger pad sliding on a vibrating plate at ultrasonic frequencies ( $> 20 \text{ kHz}$ ). It was based on a normal and a lateral spring connected to a Coulombic slider of zero mass. While it was not possible to develop an analytical solution, the model enabled the derivation of a dimensionless group,  $\Psi$ , that incorporated the governing operating and material parameters:

$$\Psi = \frac{U}{wf\mu_0(1+\nu)} \quad (1)$$

where  $U$  is the exploration velocity,  $w$  and  $f$  are the vibrational amplitude and frequency,  $\mu_0$  is the intrinsic coefficient of friction (i.e. without vibration), and  $\nu$  is the Poisson's ratio of the skin of the exploring finger pad or probe. An implication of Eq. (1) is that the performance of an ultrasonic display is independent of the elastic moduli of the *stratum corneum* and the applied normal force. This was consistent with the results of FE analyses provided that the

- T. Sednaoui, is with L2EP and ST-Microelectronics, Crolles F38920, France  
E-mail: thomas.sednaoui@st.com
- E. Vezzoli, and B. Lemaire-Semail are with Univ. Lille, Centrale Lille, Arts et Metiers ParisTech, HEL, EA 2697 - L2EP - Laboratoire d'Electrotechnique et d'Electronique de Puissance, F-59000 Lille, France  
E-mail: eric.vezzoli@ed.univ-lille1.fr, betty.semail@polytech-lille.fr
- C. Chappaz is with HAP2U, CIME NANOTECH, 3, parvis Louis NEEL 38000 Grenoble  
E-mail: cedrick.chappaz@hap2u.net
- B.Dzidek, and M. Adams are at the School of Chemical Engineering, University of Birmingham, Edgbaston, B15 2TT, United Kingdom  
Email: b.m.dzidek@bham.ac.uk, m.j.adams@bham.ac.uk

intermittent contact is sufficiently well developed; typically this corresponds to vibrational amplitudes greater than  $\sim 1 \mu\text{m}$  P-P. These analyses were carried out for a wide range of the aforementioned parameters and the data could be satisfactorily described by the following function:

$$\mu = \mu_0[1 - \exp(-\Psi/\Psi^*)] \quad (2)$$

where  $\mu$  is the actual coefficient of friction and  $\Psi^*$  is the characteristic value of  $\Psi$ . Eq. (2) satisfies the boundary conditions:  $\mu = 0$  when  $\Psi = 0$  and  $\mu = \mu_0$  when  $\Psi = \infty$ . In part 1, the experimental studies by Dai et al. [2], involving the measurement of intermittent contact of a finger pad at two different vibrational amplitudes using an optical technique, will be extended to a full characterisation of the entire relevant vibrational amplitude range. The data will be employed for calibration and validation of a finite element (FE) model that is developed in order to investigate how intermittent contact would act to reduce the friction. On the basis of the friction reduction mechanism identified by the FE model, a simplified spring-slider model will be developed. It allows a dimensionless group to be identified that incorporates the critical design, operational and user variables that govern the performance of an ultrasonic haptic display. In this work, experimental data will be described showing that a decrease in the ambient pressure does not influence the reduction in friction induced by ultrasonic vibration. This was for a limited set of experimental conditions but it does support the content that the recurrent loss in contact is a contributing mechanism. Furthermore, frictional data for human and artificial fingertips sliding on an ultrasonic plate are reported that are consistent with both the FE and spring-slider models.

## 1.2 Squeeze Film Effect

The squeeze film effect was first introduced by Watanabe et al. [5] as an explanation for the modification of the roughness perception of an ultrasonic vibrating plate by an exploring finger. A more accurate modelling of the phenomenon was proposed by Biet et al. [6] and Winter [7]. The effect relies on the generation of a thin film of over-pressurised air between a finger pad and the vibrating plate induced by the compression and decompression of the trapped air. The effective normal force, and hence the frictional force, would then be reduced, and the relative coefficient of friction given by:

$$\mu' = 1 - \frac{F_s}{F_n} \quad (3)$$

where  $F_s$  is the repulsive force resulting from squeeze film levitation and  $F_n$  is the normal force applied by the finger. By applying Reynolds equations, it is possible to define the squeeze number,  $\sigma$  [6]:

$$\sigma = \frac{12\eta wl_0}{h_0^2 p_0} \quad (4)$$

where  $\eta$  is the dynamic viscosity of air,  $l_0$  and  $h_0$  are, respectively, the length of contact and gap between the finger pad and the plate and  $p_0$  is the ambient air pressure. Details of the derivation of Eq. (4) are reported in [6]. It was suggested that a value of  $\sigma > 10$  corresponds to

the maximum overpressure,  $p_s$ , that could be achieved. This approximation allowed an analytical expression for the induced repulsive reaction force to be derived [6]. Similar results were confirmed by more accurate FE analysis [7]:

$$F_s = Ap_0(P_\infty - 1) \quad (5)$$

where  $A$  is the gross contact area between the finger pad and the plate, and  $P_\infty = p_s/p_0$  is the pressure between the finger pad and the plate induced by the squeeze film for an infinite squeeze number normalized by the ambient pressure. Thus Eq. (5) suggests that the repulsive force is linearly dependent on  $p_0$  given that  $p_s$  is not a function of  $P_\infty$  for  $\sigma > 10$ .

## 2 EXPERIMENTAL APPARATUS

### 2.1 Friction Measurements of Artificial Fingertips

#### 2.1.1 Ultrasonic Probe

Due to the extreme difficulty of performing tribological measurements under controlled conditions for a finger sliding on an ultrasonic device in a reduced pressure environment and the necessity to have a standard evaluation tool, a probe exhibiting frictional modulation similar to that of a human fingertip was developed as shown schematically in Fig. 1(a). It has a silicone elastomeric core with dimensions  $16 \times 13 \times 10 \text{ mm}$ , a Young's modulus of 1 MPa and curved edges. The contacting region was covered with a surgical tape having mechanical properties (Young's modulus of  $\sim 20 \text{ MPa}$ ) and spatial periodicity similar to that of the fingerprint ridges. To establish that the behaviour of the probe is similar to that of a human finger pad, a tribometer (TRB, CSI, Switzerland), which is shown schematically in Fig. 1(b) was used to record the frictional modulation experienced by the probe sliding on the ultrasonic device at a peak-to-peak amplitude of  $2.5 \mu\text{m}$ , a normal force of 0.5 N and an approximate exploration velocity of 17 mm/s. In addition, the velocity and acceleration of the probe and a finger pad under ultrasonic vibration were measured using the equipment described in part 1 [4] with a vibrational amplitude of  $1.35 \mu\text{m}$  and an applied normal force of 0.25 N.

#### 2.1.2 Low Pressure Friction Measurements

To quantify the influence of the squeeze film mechanism, a special tribometer and a low-pressure chamber were designed in order to investigate the evolution of the frictional modulation as a function of the ambient pressure, Fig. 1(c). The tribometer incorporated a 6-axis force sensor (nano 43, ATI, USA) that provides both lateral and normal force monitoring. The preloading of the axis can be tuned with a magnetic levitation system, and the lateral motion of the probe is actuated by a linear ultrasonic motor (M-663, PI, Germany) coupled with a driver (C-184, PI, Germany).

The vibration device is a glass plate with dimensions  $120 \times 21 \times 2 \text{ mm}$  and equipped with three piezoceramic actuators used as a driver and one as a sensor; the resonant frequency is 27.4 kHz with a stable maximum in the center of the plate and it is similar to the plates used in [8]. The pressure system consists of a cylindrical steel chamber with a detachable transparent side as shown schematically in

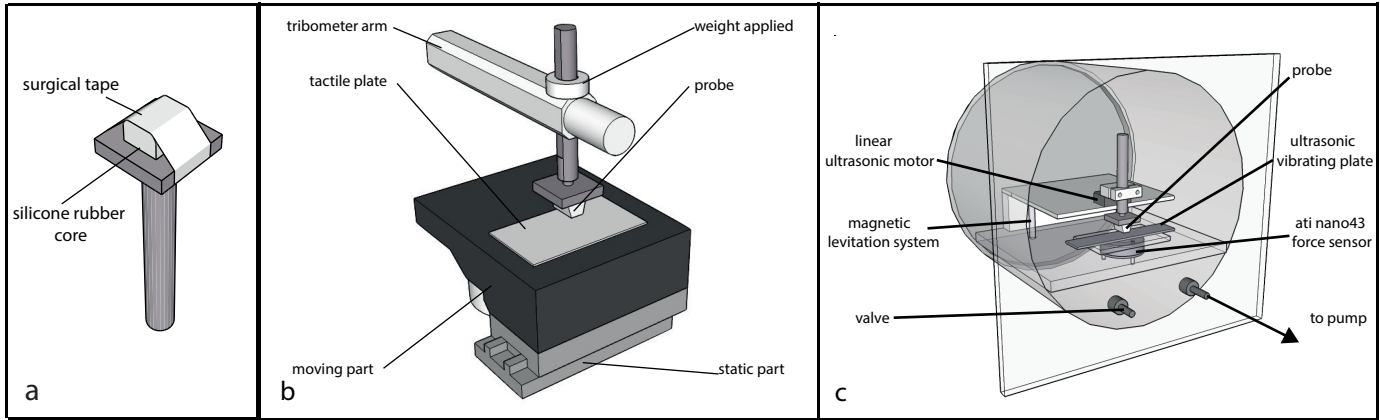


Fig. 1: Schematic diagram of (a) the artificial fingertip, (b) the tribometer for measuring the friction of artificial probes under ambient pressure, and (c) the pressure chamber for housing the tribometer and the developed low pressure tribometer.

Fig. 1(b). It was equipped with a vacuum pump (Piccolo, Thomas, Germany) and the inner pressure was measured by a manometer and regulated with a valve. It was necessary to implement a vibrational amplitude control system for the plate, which was similar to that described in [9], in order to ensure the consistency of the measurement conditions between the different atmospheric pressures. Without the control system, the reduction in the air damping on the resonator generated a significant change in the Q factor of the vibration system. This reduction, coupled with the mechanical noise induced by the friction measurements resulted in extremely unstable vibrational amplitudes of the plate. The closed-loop control implemented on the plate stabilised the vibration amplitude with a resolution of 50 nm during the friction measurements.

### 2.1.3 Measurement of the Velocity and Frequency Dependence

The tribometer described in section 2.1.1 was used to quantify the influence of the exploration velocity and vibrational frequency of the plate on the friction reduction. The plate employed for the pressure experiments was reused to measure the influence of the scanning velocity of the probe on the reduction of friction. Four different aluminium ultrasonically vibrating plates were designed by FE modelling (Salome-Mecha) to study the influence of the vibrational frequency on the reduction in friction. The plates have identical surfaces and employ the same vibrational mode but the thickness was varied in order to obtain different vibrational frequencies. Their dimensions are 41 x 76 mm with thicknesses of 1, 1.25, 1.6 and 2 mm and resonant frequencies of 36.6, 43.3, 53.7 and 66.1 kHz respectively. All the plates exhibited the same vibrational mode with a spatial wavelength of 16 mm (Fig. 2). A similar closed-loop control of the vibrational amplitude was implemented for all the plates to maintain stability of the amplitude under the range of measurement conditions investigated. A similar rough plastic film was attached to the plates in order to obtain a uniform surface roughness of  $1.23 \pm 0.03 \mu\text{m Ra}$ . During the measurement, the finger was supported by a 30 degrees finger holder and attached by double side tape on the finger nail. The vibration was measured by a piezoceramic on the

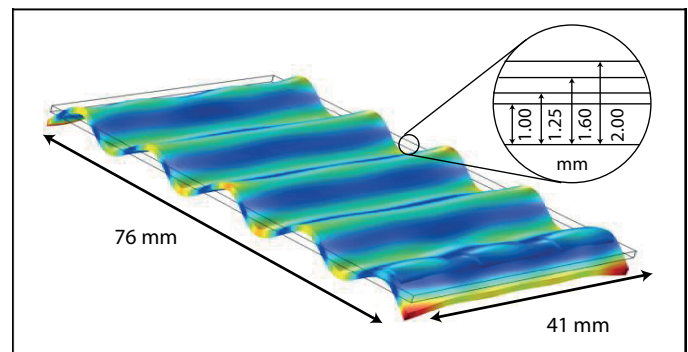


Fig. 2: Finite element representation of the vibrational mode of the aluminum plates developed for the frequency dependent study.

plate used as a sensor contextually with the vibration of the skin through the Laser Vibrometer.

## 2.2 Real Finger Pad Friction Measurements

### 2.2.1 Passive Tribometer

Previous studies of the squeeze film effect have reported measurements of the friction between a plate and a finger pad in active touch [10]. In this configuration, the finger is voluntarily exploring the surface and thus the subject is responsible for the speed of exploration and the normal force adjustment. In order to precisely control these two parameters, a passive touch based tribometer was adapted (Longshore System Engineering, Cornwall, UK) (Fig. 3a). A beam with a bearing acting as a pivot to allow free rotation is displaced laterally with a reciprocating velocity controlled by a DC motor. There is a 2-axis strain gage sensor at one end of the beam below which the vibrating plate is attached. A counterweight on a screw thread at the other end of the beam allows it to be balanced. Weights are placed on the sensor assembly to vary the normal force that is applied to the finger. An arm support provides user comfort and ergonomic control with secure wrist and hand support to allow precise finger pad positioning. A wedge-support is provided to position the finger at an angle of  $30^\circ$  to the plate. The tangential and normal forces are measured using

TABLE 1: Summary of the participants for the *in vivo* friction measurements

Participant	p1	p2	p3	p4	p5	p6
Age	27	26	32	35	30	27
Gender	F	F	F	F	M	M

two strain gauge ADC interfaces with 16-bit precision and a sampling frequency of 100 kHz implemented on a NI ADC system. The force measurements, amplitude data and position of the beam were then stored on a Windows computer using Labview and re-sampled using Matlab. Windowing was done to extract only the forces while the finger pad was located in the central region of the moving plate; data from the borders of the plates were removed to reduce the noise in the dynamic friction imposed by the triangular displacement profile of the tribometer beam.

### 2.2.2 Vibrating Plate

The vibrating device is a steel plate with dimensions 120 x 22 x 2 mm, equipped with 15 piezoceramic actuators used as a driver and one as a sensor; the resonant frequency is 25.1 kHz with a stable maximum in the center. The relationship between the voltage applied to the ceramic transducer and the generated vibrational amplitude for the mode selected was calibrated by using an interferometric vibrometer (OV-5000, Polytech, Germany) (Fig. 3b). A closed-loop system was implemented to control the vibrational amplitude of the plate to ensure the stability of the acquired data for applied normal forces  $\leq 2$  N and vibrational amplitudes  $\leq 2.5$   $\mu\text{m}$ . The mean roughness of the steel plate is  $0.36 \pm 0.03$   $\mu\text{m}$  Ra as characterised using a Surface Profiler (MicroXAM 100HR, KLA-Tencor, Belgium).

### 2.2.3 Experimental Protocol

Table 1 summarises the details of the participants for the *in vivo* friction measurements; all participants gave their informed consent. It should be noted that the measurements can be quite long and exhausting for a participant since completing a full 3D matrix for a range of velocities and loads takes a minimum of 5 h. To prevent any change in the finger pad characteristics and possible artefacts due to movements of the finger, the participants were only subjected to one parameter (velocity or normal force) for a given session. The finger to be studied was initially cleaned with a commercial soap and water and, after thorough rinsing with water, it was allowed to equilibrate for at least 10 min under ambient conditions of 16 °C and a relative humidity of 50%. The arm of the participant was positioned in the holder for the most comfortable position. The right hand index finger pad was supported by the wedge support at 30° to the horizontal and additionally adjusted by using a tape on the second phalange to prevent rotation of the finger under the high loads. Each session was initiated by automatic load calibration after which standard calibrated weights were placed on the sensor/ultrasonic plate assembly for applying the required normal force. The vibrational amplitude was increased by a staircase function in steps of 0.1 - 0.2  $\mu\text{m}$  for every three full sliding cycles.

## 3 EXPERIMENTAL RESULTS

### 3.1 Results for Artificial Fingertips

#### 3.1.1 Probe Validation

Fig. 4(a) shows the frictional forces for the probe under a normal force of 0.25 N and at a vibrational amplitude of 1.35  $\mu\text{m}$  relative to the corresponding values without vibration. It also shows published data for a human finger pad [2] and for another probe called Tango plus [3], [11] that were both acquired under approximately similar conditions to those employed for the current probe. Tango plus has an external layer mimicking the *stratum corneum* and a porous inner structure exhibiting similar viscoelastic behaviour to that of the inner tissues of the fingertip. In all cases the ultrasonic vibration induced a reduction in friction by a factor of  $\sim 4$ , thus demonstrating that the current probe is a suitable mimic for the human finger pad. This is confirmed by the results shown in Fig. 4(b) that compares the velocity and acceleration of the plate, probe and finger pad also under a normal force of 0.25 N and at a vibrational amplitude of 1.35  $\mu\text{m}$ . In terms of the phase shift relative to the plate and the magnitudes, the results are similar.

#### 3.1.2 Frictional Data at Reduced Pressure

The coefficient of friction of the probe at atmospheric and at a reduced pressure of 0.5 atm as a function of the vibrational amplitude is shown in Fig. 5 for a normal force of 0.78 N. The measurements were repeated 10 times and the RMSE is 0.002. The decrease in the coefficient of friction with increasing amplitude is similar within experimental uncertainty for both pressures. If the squeeze film effect was responsible for the reduction in friction at ambient pressure, a smaller attenuation would be expected in the reduced pressure environment; see Eq. (5).

#### 3.1.3 Frictional Data as a Function of the Vibrational Frequency, Velocity and Normal Force

Plots of the relative coefficient of friction as a function of the vibrational amplitude for the different resonant frequencies of the aluminium plates are shown in Fig. 6. The data exhibit the expected reduction in  $\mu'$  with increasing amplitude. For a given amplitude, the value of  $\mu'$  decreases systematically with increasing frequency and, at an amplitude of 3  $\mu\text{m}$ , the value at a frequency of 66.1 kHz is  $\sim 40\%$  of that at 36.6 kHz. Fig. 7 shows plots of the relative coefficient of friction as a function of the vibrational amplitude for exploration velocities in the range 25 - 100 mm/s and an applied normal force of 0.5 N. Again, the data exhibit the expected reduction in  $\mu'$  with increasing amplitude. For a given vibrational amplitude, the value of  $\mu'$  decreases systematically with decreasing exploration velocity and, at an amplitude of 3  $\mu\text{m}$ , the reduction of the friction at a velocity of 25 mm/s is a factor of  $\sim 4$  greater than that at 100 mm/s. Fig. 8 shows that the relative coefficient of friction is independent of the applied normal force for the three values examined.

### 3.2 In Vivo Friction Results

Six participants (four female and two male, mean age 29.5  $\pm$  3.5), who gave their informed consent in performing the experiment.

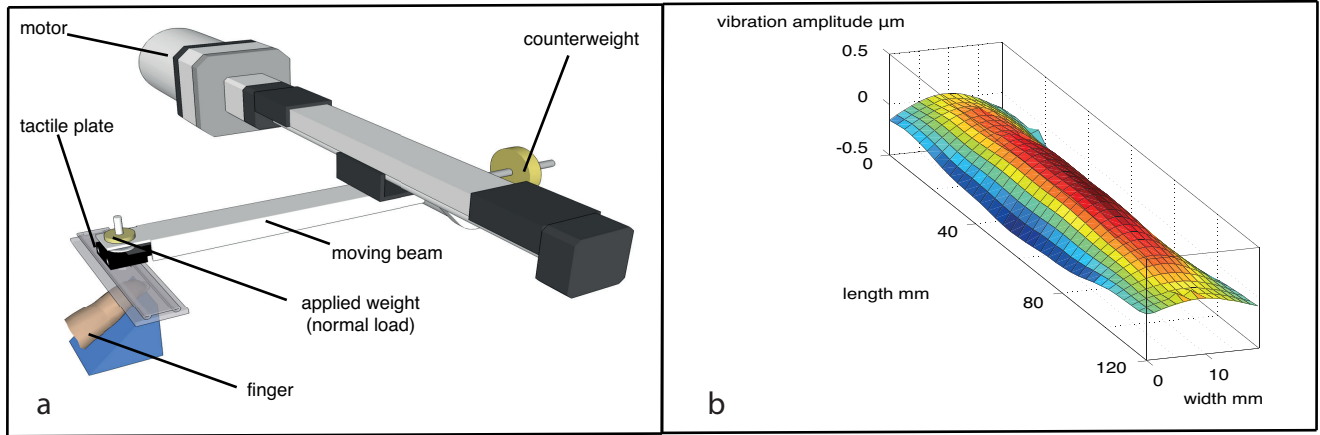


Fig. 3: (a) Schematic diagram of the reciprocating passive tribometer, (b) cartography of the vibrating steel plate as measured by an interferometric vibrometer.

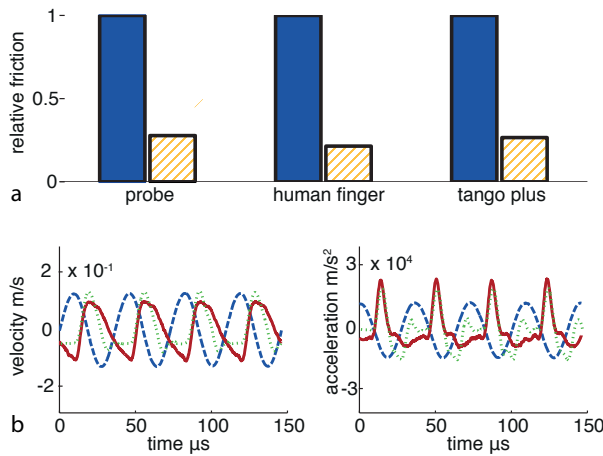


Fig. 4: (a) Comparison between the relative reduction in the friction of the current probe, a human fingertip [2] and the Tango plus probe [3], [11] due to ultrasonic vibration, where the filled and dashed bars correspond to vibration off and on respectively. (b) The velocity and acceleration of the ultrasonically vibrating plate (dashed blue line), probe (dotted green line) and finger pad (continuous red line) for a vibrational amplitude of  $1.35 \mu\text{m}$  and applied normal force of  $0.25 \text{ N}$ .

### 3.2.1 Frictional Load Index

Fig. 9 shows a plot of the frictional force for a finger pad (p1) as a function of the applied normal force at an exploration velocity of  $40 \text{ mm/s}$  measured using the passive tribometer with the plate not being vibrated. Data for the 1st cycle and for the 10th cycle are shown in Fig. 9. These preliminary results confirm that the friction coefficient between the non-vibrated ultrasonic plate and the finger is essentially independent on the normal load.

### 3.2.2 Influence of the Vibration

Previously published *in vivo* data gathered with a passive tribometer are valuable for validating the modelling presented in part 1 [4], which is a main aim of the current

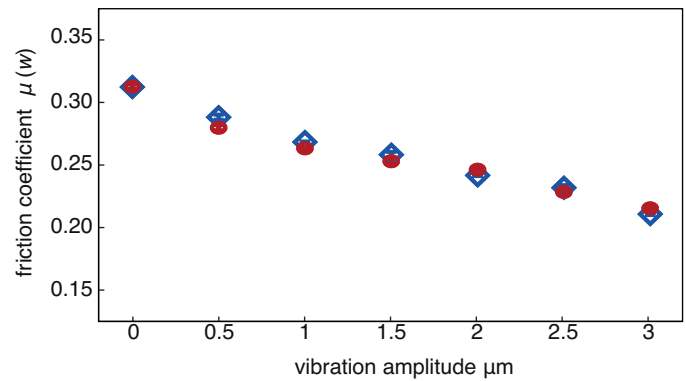


Fig. 5: The coefficient of friction of the probe as a function of the vibrational amplitude under atmospheric (blue diamonds) and reduced (red circles) pressure. A normal force of  $0.78 \text{ N}$  was applied during these tribometric measurements.

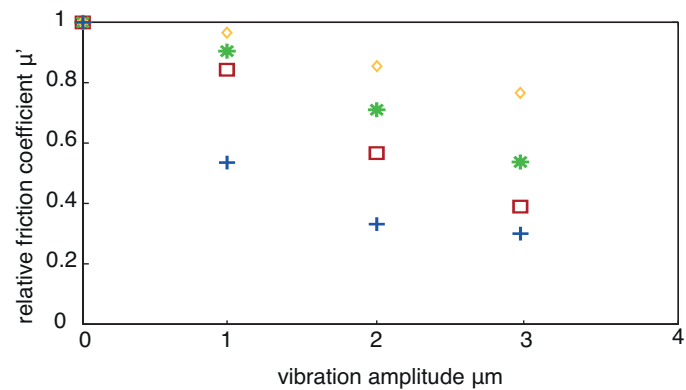


Fig. 6: The relative coefficient of friction for the probe sliding on an ultrasonic vibrating plate for an applied normal force of  $1.0 \text{ N}$  and an exploration velocity of  $30 \text{ mm/s}$ , and for vibrational frequencies of  $36.6$  (yellow diamonds),  $43.3$  (green stars)  $53.7$  (red squares) and  $66.1 \text{ kHz}$  (blue crosses).



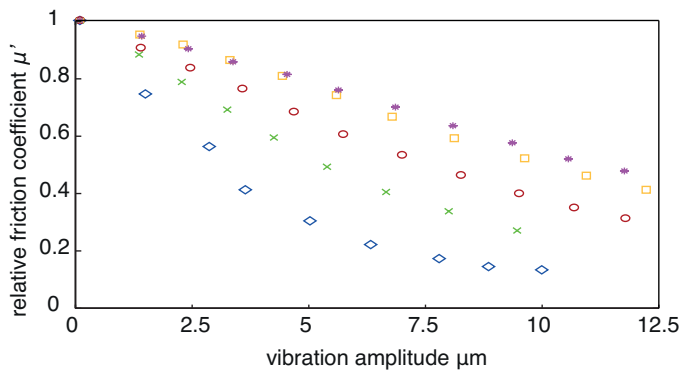


Fig. 7: The relative coefficient of friction for the probe sliding on an ultrasonic vibrating plate as a function of the vibrational amplitude for an applied normal force of 0.5 N and vibrational frequency of 25.1 kHz. The exploration velocities are 10 (blue diamonds), 25 (green crosses), 50 (red circles), 75 (yellow squares) and 100 mm/s (purple stars).

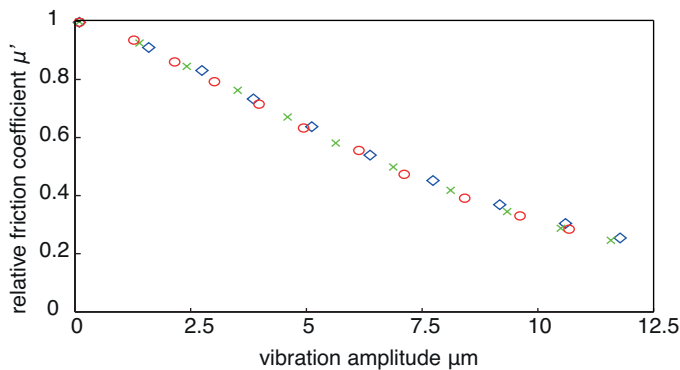


Fig. 8: The relative coefficient of friction for the probe sliding on an ultrasonic vibrating plate as a function of the vibrational amplitude for applied normal forces of 0.25 N (blue diamonds), 0.5 N (green crosses), and 0.75 N (red circles), with an exploration velocity of 25 mm/s, and vibrational frequency of 25.1 kHz.

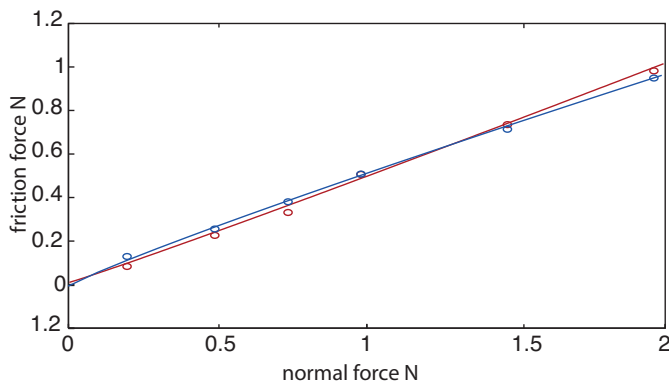


Fig. 9: The frictional force as a function of the applied normal force for a finger pad with an exploration velocity of 40 mm/s for the 1st exploration cycle (red) and the 10th cycle (blue). The lines are the best fit to (7).

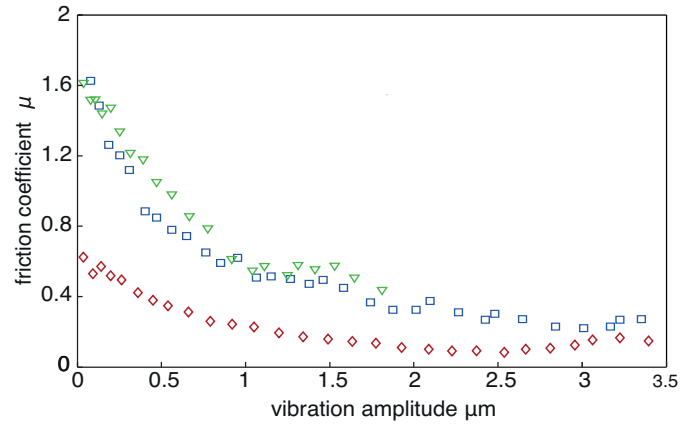


Fig. 10: Literature data [8] for the coefficient of friction as a function of vibrational amplitude at a frequency of 25.1 kHz and an exploration velocity of 17 mm/s for three different participants with applied normal forces of  $\sim 0.1$  N.

paper. Consequently, it will be included in this section for convenience. Fig. 10 shows such data [8] for the coefficient of friction as a function of the vibrational amplitude at a frequency of 25.1 kHz and an exploration velocity of 17 mm/s for three different participants and a similar applied normal force of  $\sim 0.1$  N. It exemplifies the wide variation in the absolute coefficients of friction for different participants.

Similar data measured in the current work are presented in Fig. 11(a) for one participant (p5) with an applied normal force of 0.5 N, and a vibrational frequency of 25.1 kHz for three exploration velocities of 20, 40 and 80 mm/s. The reduction in the friction is systematically greater with decreasing exploration velocity. Comparable trends for the dependency of the vibrational amplitude are evident in Fig. 11(b) from a normalization of the data shown in Fig 10, but this was for a single exploration velocity of 17 mm/s. An important point about Fig. 11(b) is that normalisation results in an approximate superposition of the data. The mean values of the relative coefficient of friction as a function of the vibrational amplitude for all participants are presented in Fig. 12. There is not a systematic dependence on the applied normal force for the range examined.

## 4 DISCUSSION

On the basis of FE modelling, it was argued that the reduction in friction for ultrasonic haptic displays could be ascribed to a ratchet mechanism in which engagement induces lateral deformation of the fingerprint ridges, or the contacting surface in the case of artificial probes, until the frictional mobilisation criterion is satisfied [4]. Thus during any vibration cycle, the friction is either (i) zero when there is a loss of contact or (ii) less than the slip value. The model was evaluated in the current work by calculating the influence of the vibrational amplitude for a range of exploration velocities and normal forces for *in vivo* and probe frictional data.

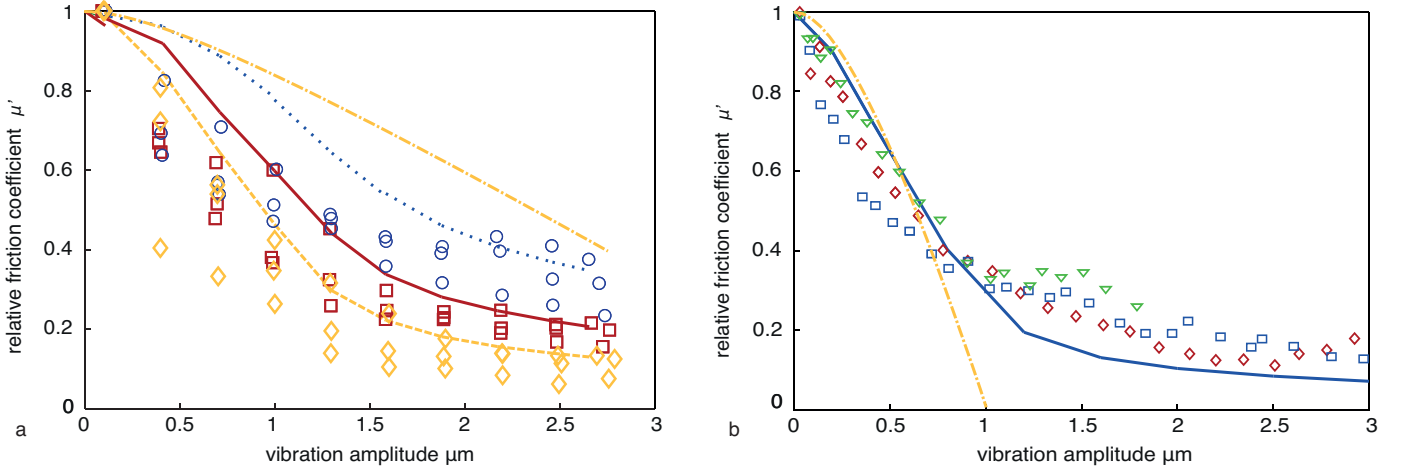


Fig. 11: (a) The relative coefficient of friction for p5 as a function of the vibrational amplitude at a frequency of 25.1 kHz, an applied normal force of 0.5 N and the following exploration velocities: 20 (yellow diamonds), 40 (red squares) and 80 (blue circles) mm/s. The dashed yellow line, red line, and blue dotted line are, respectively, the prediction of the FE model [4] of the friction reduction in the experimental condition. (b) Literature data for an applied normal force of 0.10 N for three different subjects (red diamonds, blue squares, and green triangles), exploration velocity of 17 mm/s and the vibrational frequency of 25.1 kHz [8], compared with the FE model prediction (blue line) [4]. The yellow chain lines was calculated using the squeeze film model [6].

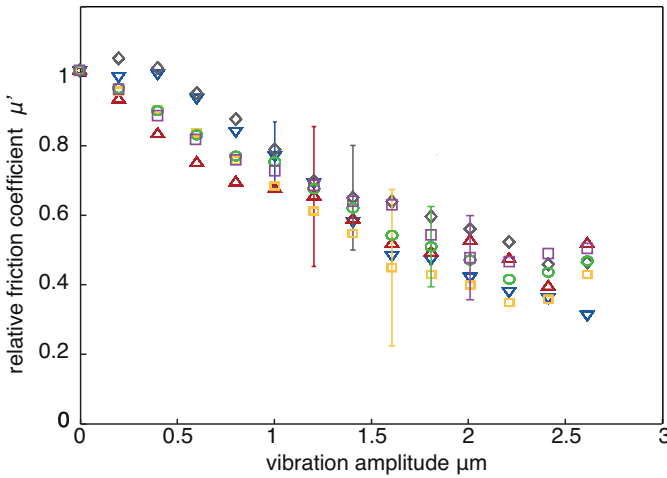


Fig. 12: Mean relative coefficient of friction for all participants (p1 - p6) as a function of the vibrational amplitude for the following applied normal forces: 0.2 (blue down triangle), 0.5 (red up triangle), 0.75 (grey diamonds), 1.0 (yellow squares), 1.5 (green circles), and 2 N (purple left triangles). The error bars indicate the mean standard deviation between the participants.

## 4.1 Mechanical Model Validation

### 4.1.1 Velocity and Frequency Influence

The calculated values of  $\mu'$  with the FE model are compared with the experimental data in Fig. 11 and the trends in the numerical values are reasonably similar to those measured despite the model being relatively simple. The self-consistency of the FE results and the dimensionless group derived from the spring-slider model was demonstrated by showing that this group could be used to satisfactorily superimpose the numerical results applied to a finger pad [4].

However, at vibrational amplitudes smaller than  $\sim 1 \mu\text{m}$  the intermittent contact may be insufficiently developed for the friction not to be influenced by the Young's modulus of the *stratum corneum* and the applied normal force, depending on the vibrational frequency. This is the case for the reduced variables plot of the *in vivo* data given in Fig. 13. There is reasonable data superposition for vibration amplitudes  $> 1 \mu\text{m}$  and these data were fitted to the exponential function (2) with  $\Psi^* = 4.69 \pm 0.32$  as shown in the figure. This value of  $\Psi^*$  is greater than that ( $2.38 \pm 0.21$ ) for the FE analysis of a finger pad, but it reflects the greater scatter of *in vivo* measurements of ultrasonic displays and, in particular, the small range of the dimensionless group that could be fitted. In comparison, using the probe, it is possible to achieve data superposition for a range of vibrational frequencies, and exploration velocities as well as vibrational amplitudes (Fig. 14) since the minimum vibrational amplitude is  $1 \mu\text{m}$ . In this case, the value of is  $0.70 \pm 0.04$ .

It is of interest that the boundary condition assumption of  $\mu = 0$  when  $\Psi = 0$  in the derivation of Eq. (2) seems to satisfy the experimental data rather than a finite value of  $\mu$  at  $\Psi = 0$ . This suggests that the performance of ultrasonic displays could be improved further by increasing the vibrational frequency to values that are greater than those examined in the current work, due to the dependence of  $\Psi$  on this variable.

### 4.1.2 Influence of the Applied Normal Force

Fig. 8 and the fit reported in Fig. 14 show that for the artificial fingertip there is no influence on  $\mu'$  of the applied normal force, and consequently for the value of  $\Psi^*$ . However, as discussed previously, *in vivo* data are considerably more scattered and less reproducible as exemplified in Fig. 15 for two of the participants and a range of applied normal forces. A possible contributory factor is that the finger pads exhibited a wide range of Young's moduli so that not all



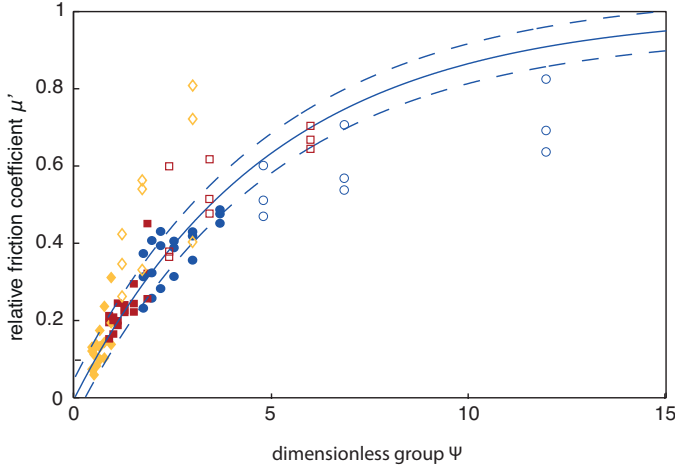


Fig. 13: Relative friction for participant p5 with an exploration velocity of 20 (yellow diamonds), 40 (red squares) and 80 mm/s (blue circles) as a function of the dimensionless group; the data are taken from Fig. 11(a). The full line is the best fits of the filled points to Eq. (2) and the value of  $\Psi^*$  is  $4.69 \pm 0.32$ ; the unfilled points correspond to  $w < 1 \mu\text{m}$  and were not included in the fit, as the dimensionless group is not relevant for small amplitude of vibration. The dashed lines show the RMSE variation of the fit.

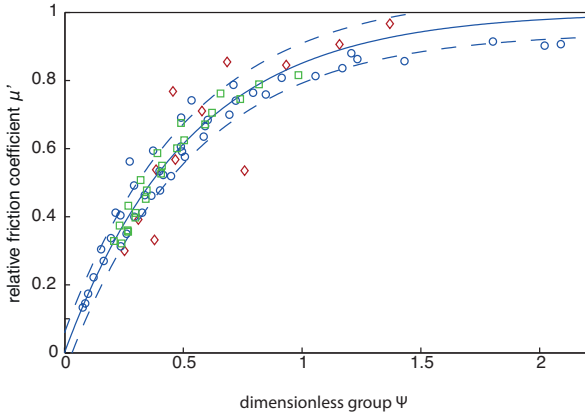


Fig. 14: The relative coefficient of friction as a function of the dimensionless group for the probe sliding on an ultrasonic vibrating plate with a range of vibrational frequencies (red diamonds), exploration velocities (blue circles) and applied normal forces (green squares) the data are taken from Figs 6, 7 and 8 respectively. The full lines are the best fits to Eq. (2) and the value of  $\Psi^*$  is  $0.70 \pm 0.04$ ; the dashed lines correspond to the RMSE variation.

the data corresponded to the intermittent contact being sufficiently well developed. In such cases, the dimensionless group approach becomes inapplicable at smaller vibrational amplitudes. However, by taking mean values of the data for all participants (Fig. 12) and fitting to the exponential function, mean values of  $\Psi^*$  as a function of the applied normal force were obtained (Fig. 16). The figure shows the best fit to a linear relationship with a slope of  $-0.094$  with 95% confidence bounds of  $-0.49$  and  $0.30$  and an intercept of  $1.80$  with 95% confidence bounds of  $1.34$  and  $2.27$ . Thus it

may be concluded from these data that  $\Psi^*$  is not a strong function of the applied normal force and that the mean value of  $\Psi^*$  is reasonably consistent with that of the numerical data for which  $\Psi^* = 2.38 \pm 0.21$  [4].

The FE model employed a Coulombic boundary condition:

$$F_l = \mu_0 F_{\text{reac}} \quad (6)$$

where  $F_l$  is the lateral force and  $F_{\text{reac}}$  is the normal reaction force of the vibrating plate. However, a finger pad exhibits non-Coulombic friction against smooth surfaces [12], [13]:

$$F_l = k_f F_{\text{reac}}^n \quad (7)$$

where  $k_f$  is the friction factor and  $n$  is the frictional load index with  $2/3 \leq n \leq 1$ . Consequently, Eq. (1) could be generalised as follows:

$$\Psi = \frac{U F_{\text{reac}}^n}{k_f w f \mu_0 (1 + \nu)} \quad (8)$$

where  $k_{f0}$  is the intrinsic value of  $k_f$ . The data in Fig. 9 were fitted to Eq. (7) with  $F_{\text{reac}} = F_n$  since the plate was in a static state, with  $k_f = 0.49 \pm 0.02$  and  $n = 1.05 \pm 0.08$  for the 1st cycle and  $k_f = 0.52 \pm 0.01$  and  $n = 0.91 \pm 0.05$  for the 10th cycle. The dependence of the friction on the applied normal force may be understood because the friction of human skin is described by the adhesion mechanism [12]. That the value of  $n$  is approximately unity probably arises because the stainless steel plate used for the *in vivo* friction measurements is not optically smooth and it is known that topographically rough surfaces exhibit such Coulombic behavior [13].

In principle, the dimensionless group should be modified according to Eq. (8) but the current data strongly suggest that the *in vivo* and the artificial fingertip friction modulation is not a function of the applied normal force. Thus Eq. (1) is the better descriptor of the phenomenon for both *in vivo* and probe measurements. This is probably a consequence of the friction modulation being primarily governed by the deformation of the fingerprint ridges and the extent to which there is a loss in contact rather than being dominated by slip for which the adhesion mechanism would apply.

## 4.2 Squeeze Film Effect

The values of  $\mu'$  calculated using the squeeze film model [6] are also shown in Fig. 11. The experimental data fit less closely and the model cannot account for the friction being a function of the exploration velocity. Moreover, these findings are consistent with the observation that the friction is not influenced by a reduced ambient pressure in the case of the artificial probe (Fig. 5). The interplay between the frictional ratchet mechanism demonstrated in this paper and the recent measurements suggesting a role of the squeeze film effect [14] is outside of the scope of the current work, and will be the subject of future investigations. Indeed, an initial study of the contribution of the squeeze film effect to the attenuation of friction was performed by Vezzoli et al. [15]. The result obtained in this study, which dealt with a real finger in reduced pressure, was a partial decrease in friction reduction as a function of the pressure. This behavior may suggest a combination of both effects. However,

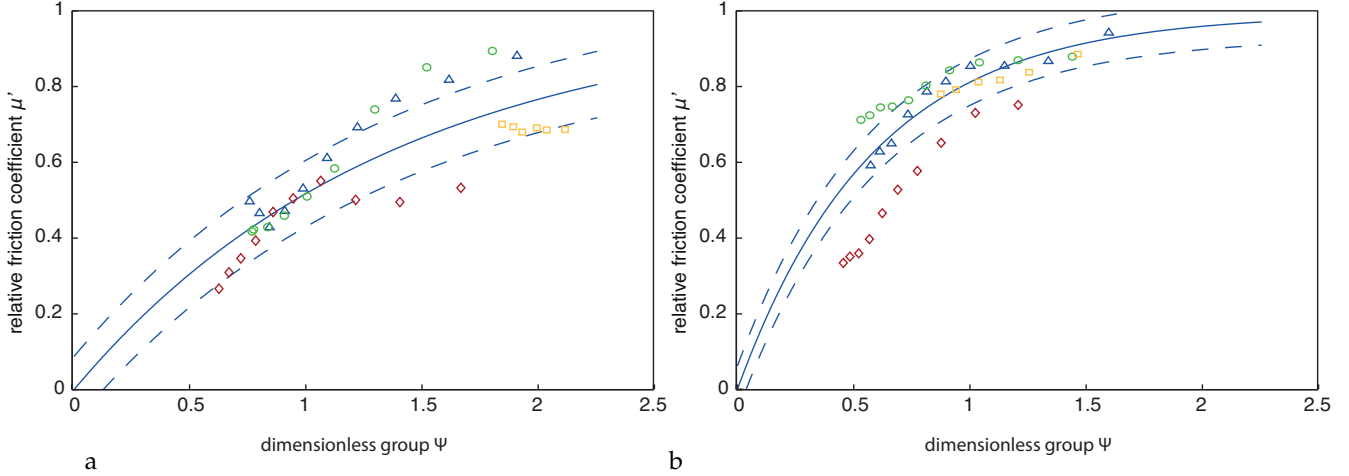


Fig. 15: The relative coefficient of friction as a function of the dimensionless group measured for two participants with an exploration velocity of 40 mm/s and a range of normal forces. (a) p2: 0.75 (red diamonds), 1 (blue triangle), 1.5 (green circles) and 2 N (yellow squares). (b) p3: 0.2 (red diamonds), 0.75 (blue triangle), 1 (green circle), and 2 N (yellow squares). The full lines are the best fits to Eq. (2) and values of  $\Psi^*$  equal to  $1.89 \pm 0.18$  and  $0.78 \pm 0.046$  respectively; the dashed lines correspond to the standard deviation of the fit to the exponential function (2).

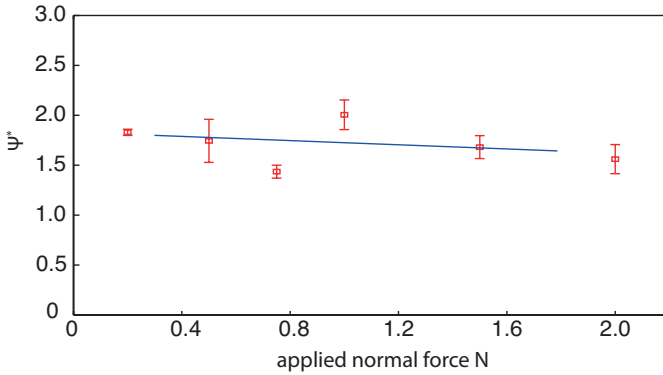


Fig. 16: The characteristic value of the dimensionless group as a function of the applied normal force calculated by fitting Eq. (2) to the data in Fig. 12. The line is the best linear fit to the data.

it was clear that the more refined methodology reported here is necessary to avoid complications due to the possible influence of the reduced pressure on the mechanical and frictional properties of the skin.

## 5 CONCLUSION

The current experimental data are consistent with the FE model developed in part 1 [4] and also the data superposition scheme derived in that work. Thus, the proposed ratchet mechanism is a satisfactory explanation for the friction modulation of ultrasonic displays. In particular, the friction modulation depends on the exploration velocity and is independent of the applied normal force and, in the case of the current probe, independent on the ambient air pressure. On the basis of the current work, it is not possible to quantify the relative contribution of squeeze film levitation. Data reduction using an exponential function of

a dimensionless group shows a reasonable description of experimental data, provided that the intermittent contact is sufficiently well developed. This requires that the vibrational amplitude must be  $> 1 \mu\text{m}$  for the range of frequencies examined here. Another important point confirmed by this work is the influence of the vibrational velocity on the reduction of friction, not the simple vibrational amplitude ( $fw$ ).

## ACKNOWLEDGMENTS

The Authors acknowledge FP7 Marie Curie Initial Training Network PROTOTOUCH (grant agreement No. 317100) for funding, and the IRCICA laboratory for hosting.

## REFERENCES

- [1] M. Biet, G. Casiez, F. Giraud, and B. Lemaire-Semail, "Discrimination of virtual square gratings by dynamic touch on friction based tactile displays," in *Symposium on Haptic interfaces for virtual environment and teleoperator systems*, 2008, pp. 41–48.
- [2] X. Dai, J. Colgate, and M. Peshkin, "LateralPaD: A surface-haptic device that produces lateral forces on a bare finger," in *2012 IEEE Haptics Symposium (HAPTICS)*, Mar. 2012, pp. 7–14.
- [3] R. Fenton Friesen, M. Wiertelowski, and J. E. Colgate, "The role of damping in ultrasonic friction reduction," *IEEE - Haptic Symposium 2016*, pp. 167–172.
- [4] E. Vezzoli, Z. Vidrih, V. Giamundo, B. Lemaire-Semail, F. Giraud, T. Rodic, D. Peric, and M. Adams, "Friction reduction through ultrasonic vibration: Part 1: Modelling intermittent contact and friction reduction," *Submitted to IEEE Transaction on Haptics*, 2016.
- [5] T. Watanabe and S. Fukui, "A method for controlling tactile sensation of surface roughness using ultrasonic vibration," in *IEEE International Conference on Robotics and Automation, Proceedings*, vol. 1, May 1995, pp. 1134–1139 vol.1.
- [6] M. Biet, F. Giraud, and B. Lemaire-Semail, "Squeeze film effect for the design of an ultrasonic tactile plate," *IEEE Transactions on Ultrasonics, Ferroelectrics, and Frequency Control*, vol. 54, no. 12, pp. 2678–2688, Dec. 2007.
- [7] C. Winter, "Friction feedback actuators using squeeze film effect," Ph.D. dissertation, Ecole Polytechnique Federale de Lausanne, 2014.

- [8] T. Sednaoui, E. Vezzoli, B. M. Dzidek, B. Lemaire-Semail, C. Chiappaz, and M. Adams, "Experimental evaluation of friction reduction in ultrasonic devices," in *IEEE - World Haptics Conference 2015*, 2015, pp. 37–42.
- [9] W. Ben Messaoud, B. Lemaire-Semail, M.-A. Bueno, M. Amberg, and F. Giraud, "Closed-loop control for squeeze film effect in tactile stimulator," *Actuator 2014*.
- [10] L. Winfield, J. Glassmire, J. Colgate, and M. Peshkin, "T-pad: Tactile pattern display through variable friction reduction," in *EuroHaptics Conference and Symposium on Haptic Interfaces for Virtual Environment and Teleoperator Systems. World Haptics 2007. Second Joint*, 2007, pp. 421–426.
- [11] R. Fenton Friesen, M. Wiertlewski, M. A. Peshkin, and J. E. Colgate, "Bioinspired artificial fingertips that exhibit friction reduction when subjected to transverse ultrasonic vibrations," *IEEE - World Haptics Conference 2015*.
- [12] M. J. Adams, S. A. Johnson, P. Lefèvre, V. Lévesque, V. Hayward, T. André, and J.-L. Thonnard, "Finger pad friction and its role in grip and touch," *Journal of The Royal Society Interface*, vol. 10, no. 80, 2012.
- [13] B. M. Dzidek, M. Adams, Z. Zhang, S. Johnson, S. Bochereau, and V. Hayward, "Role of occlusion in non-Coulombic slip of the finger pad," in *Haptics: Neuroscience, Devices, Modeling, and Applications*, ser. Lecture Notes in Computer Science, M. Auvray and C. Duriez, Eds. Springer Berlin Heidelberg, Jan. 2014, pp. 109–116.
- [14] M. Wiertlewski, R. Fenton Friesen, and J. E. Colgate, "Partial squeeze film levitation modulates fingertip friction," *Proceedings of the National Academy of Sciences*, vol. 113, no. 33, pp. 9210–9215, 2016. [Online]. Available: <http://www.pnas.org/content/113/33/9210.abstract>
- [15] E. Vezzoli, W. Ben Messaoud, F. Giraud, and B. Lemaire-Semail, "Pressure dependence of friction modulation in ultrasonic devices," *World Haptics Conference (WHC)*, 2015.

**Cedrik Chappaz** Cedrick Chappaz obtained his PhD degree of Physics from Universit de Besanon in 2003. He held various positions inside R&D department from STMicroelectronics, semiconductor company. Since 2015, he is CEO of HAP2U, a company delivering ultrasonic solutions for touch interfaces.

**Thomas Sednaoui** Sednaoui got a double MS degree in aerospace engineering from IPSA (Paris, France) and SAU University (Shenyang, China) in 2010. He worked at the European Space Agency (ESA) - Telerobotic & Haptic Lab to develop exoskeletons haptic system for teleoperation for ISS Experiment. From October 2013 he is employed by STMicroelectronics and doing his PhD Thesis with the ITN Prototouch Project. His research focuses on the understanding and industrialisation of ultrasonic devices.

**Michael Adams** was awarded a PhD in molecular acoustics from the University of Essex, UK and is Professor of Product Engineering and Manufacturing in the School of Chemical Engineering at the University of Birmingham, UK since 2004 and was previously a Senior Scientist with Unilever R&D. He is a Fellow of the UK Royal Academy of Engineering. He was the recipient of the Donald Julius Groen Prize (IMechE) for outstanding achievements in interfacial engineering. His research interests include the friction of human skin and applications to tactile sensors and displays.

**Eric Vezzoli** got his MS degree in Physics Engineering from the Politecnico di Milan (Italy) in 2013. From September 2013 he is research assistant at L2EP-IRCICA Laboratory working on his PhD Thesis with the ITN Prototouch Project. His domain of research are tactile stimulation principle modelling, tactile display designing and tactile perception.

**Brygida Dzidek** Studied Materials Science Engineering from the University of Silesia (Poland). She gained research experience working in Swiss Federal Laboratories for Materials Science and Technology (EMPA) developing new biomaterials and electro-ceramic composites. From September 2013 she is a Research Fellow in the School of Chemical Engineering at Birmingham University carrying out her work within the EU funded ITN Prototouch.

**Betty Lemaire-Semail** received the Ph.D. degree in 1990 from the University of Paris XI, Orsay. From 1990 to 1998, she was an assistant professor at the Ecole Centrale of Lille and she is now a professor at the University Lille 1. Her main field of interest now deals with the modeling and control of piezoelectric actuators for positioning and force feedback applications.